JOURNAL OF CATALYSIS **179,** 43–55 (1998)
ARTICLE NO. CA982176

# Comparative Study of *n*-Hexane Aromatization on Pt/KL, Pt/Mg(Al)O, and Pt/$SiO_2$ Catalysts: Clean and Sulfur-Containing Feeds

Gary Jacobs, Cristina L. Padro, and Daniel E. Resasco[1]

*School of Chemical Engineering and Materials Science, University of Oklahoma, 100 E. Boyd Street, Norman, Oklahoma 73019*

Received December 11, 1997; revised June 4, 1998; accepted June 8, 1998

**The *n*-hexane aromatization has been studied on Pt/KL, Pt/Mg(Al)O, and Pt/$SiO_2$ catalysts at 773 K using sulfur-free and 0.6 ppm sulfur containing feedstocks. Examination of the product distribution as a function of conversion suggests that the formation of benzene is preceded by the formation of hexenes. In contrast with previous reports, it has been found that the Pt/KL catalyst exhibits much higher aromatization activity than the Pt/Mg(Al)O catalyst. On Pt/KL the main product is benzene, with hexenes and lighter compounds as the principal by-products. By contrast, on the Pt/Mg(Al)O, the main products were hexenes. Since hexenes are primary products and benzene is a secondary product, the exceptional aromatization activity of Pt/KL is explained in terms of its ability to convert hexene into benzene. In the presence of sulfur, the Pt/KL exhibits a rapid loss in *n*-hexane conversion and benzene selectivity. Under these conditions, the sulfided Pt/KL catalyst presents a catalytic behavior typical of Pt/Mg(Al)O and Pt/$SiO_2$, generating larger amounts of hexenes. The observed results are consistent with the hypothesis that the most important role of the zeolite is to inhibit bimolecular interactions that lead to coke formation. The formation of coke has the net effect of selectively deactivating aromatization sites which require a large ensemble of atoms to constitute the active site but not affecting the dehydrogenation activity which is less ensemble-sensitive. Therefore, those particles that are not protected against coking inside the channels of the zeolite rapidly become unselective. In support of this hypothesis, the hydrogenolysis reaction which also requires a large ensemble of atoms, decreases in parallel with the aromatization reaction. The high sensitivity of Pt/KL to sulfur may be due to a combination of effects which may involve growth of metal particles outside the zeolite which would become unselective and partial poisoning of the particles inside the zeolite, causing a similar selective deactivation.** 

## INTRODUCTION

The exceptionally high activity and selectivity exhibited by Pt/KL zeolite catalysts for the aromatization of *n*-hexane to benzene are well established (1–4) and have lead to the development of successful commercial processes (5). However, a major shortcoming for these catalysts is their extremely high sensitivity to even minute concentrations of sulfur (e.g., parts per billion), requiring very expensive and complicated sulfur-removal operations. Therefore, for years there has been a strong interest in finding catalysts able to effect the aromatization reactions in the presence of sulfur.

Although it is well accepted that the aromatization reaction on these catalysts is monofunctional, the fundamental reasons for both their exceptional catalytic properties and their high sulfur sensitivity are still unresolved. Several possible explanations about the high aromatization activity have been considered (6). Among them, some explanations ascribe the unique features of the Pt/KL catalysts to structural parameters of the L zeolite (7), while other explanations focus on its basicity (8), or a combination of both. One of the early explanations was that, through nonbinding interactions, the microporous structure favored particular molecular arrangements that lead to aromatization (9). More recent studies have proposed that the L zeolite structure and its lack of acidity inhibit coke formation by bimolecular encounters (10, 11). Other authors have proposed that the small Pt particles inside the channels of the basic zeolite are electron rich and, consequently, exhibit unique catalytic properties (12). These interactions would be responsible for the stabilization of very small Pt particles (13) that would remain inside the channels of the zeolite, even at the high temperatures required for the aromatization reaction.

Despite the great disparity in the possible explanations offered by several authors, most of them agreed in the uniqueness of the L zeolites to promote high aromatization selectivity. However, a surprising result was reported in 1991 (14). It was found that using Pt catalysts supported on Al-stabilized MgO, the *n*-hexane conversion at a given contact time, as well as the aromatization selectivity at a given conversion, was almost identical to those obtained on a Pt/KL catalyst under the same conditions. This result would certainly disfavor any explanation that involves the role of the L zeolite structure as being mainly responsible for the aromatization activity, since the Mg(Al)O support is not microporous. Consequently, this result gave strong support to theories promoting the idea that the basicity of

[1] To whom correspondence should be sent. E-mail: resasco@ou.edu.



0021-9517/98 $25.00

the support was the essential feature and the main role of the support was to electronically modify the Pt particles. Nevertheless, more recent results have suggested that in fact Pt/Mg(Al)O may not be nearly as active and selective as Pt/KL (13, 15). In this investigation we are making a direct comparison of the two materials under several conditions to help resolve the conflicting reports. In addition to the Pt/KL and Pt/Mg(Al)O catalysts, we have studied a $Pt/SiO_2$ catalyst as a nonmicroporous reference material, in which minimal metal–support effects should be expected.

The second important part of our study is the sensitivity to sulfur. As mentioned above, one of the most serious drawbacks exhibited by the Pt/KL catalysts is their low sulfur tolerance. It is our interest to determine whether Pt/Mg(Al)O has the same high sensitivity to sulfur as Pt/KL, or if it is more resistant and can have potential as a practical catalyst.

## EXPERIMENTAL

### 1. *Catalytic Materials*

Three support materials were used in this study. The K-LTL zeolite (series TSZ-500, BET area 292 $m^2/g$, $SiO_2/Al_2O_3$ ratio = 6) was provided by Tosoh Company. Before addition of the metal, the K-LTL zeolite was dried in an oven at 373 K for 12 h and calcined at 673 K for 5 h. The Al-stabilized magnesium oxide support, Mg(Al)O, was prepared by coprecipitation of aluminum nitrate and magnesium nitrate from an aqueous solution at 333 K–348 K, following the procedure reported in previous studies (14, 16–17). The Mg/Al ratio in the solution was kept at 5 : 1 and the total cation concentration was 1 *M*. A potassium hydroxide–potassium carbonate solution was prepared to keep a molar ratio of $CO_3^{2-}/Al = 0.5$ while potassium hydroxide solution was required to keep the pH stable at 9. The filtrate was washed with ultrapure water and dried first at room temperature for 10 h, and then placed in an oven at 383 K for 24 h. The dried sample was calcined at 873 K in air for 12 h (BET area 150 $m^2/g$, average pore radius 100 Å). The material was characterized during several stages in the synthesis process using XRD and it was confirmed that at every stage the structure was the same as those reported in previous work (18). The $SiO_2$ support employed in this study was a silica gel (Davison Grade 923) provided by W. R. Grace.

The incorporation of the platinum was realized by two methods. In the first method, incipient wetness impregnation (IWI) of the support was performed with platinum salt tetraammineplatinum(II) nitrate (Alfa, Stock #88960, Lot #H24F22). The liquid/solid ratios were determined for each support to obtain the same degree of incipient wetness in all catalysts. After impregnation, the samples were dried overnight at 383 K. Subsequently, they were heated at a rate of 3K/min up to 623 K in an air flow of 100 $cm^3/min\ g_{cat}$. They were kept at the same temperature and air flow for 2 h.

**TABLE 1**

**Catalyst Characteristics**

| Catalyst | BET surface area ($m^2$/gram) | Pore radius (angstroms) | Preparation method | Amount of Pt (wt%) |
|---|---|---|---|---|
| Pt/KL (IWI) | 292 | 7.1 (min.), 13 (max.) | IWI | 1 |
| Pt/KL (VPI) | 292 | 7.1 (min.), 13 (max.) | VPI | 1 |
| Pt/Mg(Al)O | 100 | Ave. 100 | IWI | 1 |
| $Pt/SiO_2$ | 470 | Ave. 25 | IWI | 1 |

The second method was vapor phase impregnation (VPI) (13). In this case, the KL zeolite was calcined for 5 h at 673 K to remove chemisorbed water. In an inert atmosphere, $Pt(AcAc)_2$ was physically well-mixed with the KL, and the solid mixture was loaded into a reactor tube. The reactor tube was sealed under vacuum and evacuated overnight to 0.02 Torr. The catalyst was then slowly ramped to 333 K and held there for 1 h to remove impurities. The material was then slowly ramped to 373 K and held for 1 h to sublime the $Pt(AcAc)_2$, at which temperature the pressure increased substantially. After sublimation, the catalyst was ramped to 423 K and held for 15 min to ensure that virtually all of the $Pt(AcAc)_2$ was sublimed. At this point, the sample was yellow in color, indicating that the $Pt(AcAc)_2$ did not decompose during the procedure. To decompose the precursor, the sample was ramped to 623 K in flow of air for 2 h and calcined at 623 K for 2 h. The characteristics of the four catalysts investigated are summarized in Table 1.

### 2. *Catalyst Characterization*

The surface areas and pore size distributions of the supports were determined using an adsorption unit ASAP 2010 from Micromeritics. Transmission electron microscopy (TEM) images were obtained in a JEOL 200FX-TEM on all fresh catalysts and after they were exposed to reaction conditions using sulfur-free feed and feed containing 0.6 ppm sulfur.

Fresh and spent samples were characterized by EXAFS spectroscopy at the National Synchrotron Light Source (NSLS) at Brookhaven National Laboratory, Upton, New York, using beam line X-18b equipped with a Si (111) crystal monochromator. The X-ray ring at the NSLS has an energy of 2.5 GeV and a ring current of 80–220 mA. After reduction in flowing $H_2$ at 773 K, EXAFS data were taken near the $L_{III}$-edge of Pt (11,564 eV). The experiments were conducted in a stainless steel sample cell, which allowed *in situ* treatments in a $H_2$ or He atmosphere at temperatures ranging from 773 K to liquid nitrogen temperature. Before each measurement, the fresh or previously used catalysts were re-reduced *in situ* at 573 K (heating ramp of 10K/min) for 30 min in flowing $H_2$. The EXAFS spectra were recorded at liquid nitrogen temperatures in the presence of $H_2$. Six scans were recorded for each sample. The average spectrum

was obtained by adding the six scans. The preedge background was subtracted by using power series curves. Subsequently, the postedge background was removed using a cubic spline routine. The spectra were normalized by dividing by the height of the absorption edge. To avoid overemphasizing the low energy region (19), the $\chi$ data were $k^3$-weighted. The range in $k$-space utilized to do the analysis was 3.5–15 $Å^{-1}$. Theoretical references for Pt-Pt, Pt-S, and Pt-O bonds were obtained by using the FEFF program from the University of Washington (20–22). The FEFFIT fitting routine was employed to obtain the structural parameters of the Pt clusters after the various thermal treatments on the different supports. The Debye Waller factors for each bond type ($\sigma$), the edge energy difference ($\Delta E_o$), the coordination number N, and the difference in bond distances ($\Delta R$) with respect to the theoretical reference, were used as fitting parameters.

### 3. *Catalytic Activity*

Catalytic reaction tests were conducted at atmospheric pressure using two fixed-bed, single pass, and continuous-flow reactors in parallel. One reactor was only used for clean *n*-hexane runs, while the other reactor was only used for sulfur deactivation studies. To avoid contamination of the clean runs, all lines leading to each reactor were kept segregated. Each reactor consisted of a 0.5-inch stainless steel tube with an internal K-type thermocouple. The oven was controlled with a J-type thermocouple. The experiments were conducted using between 0.10 and 0.40 g of catalyst in each run. Each catalyst was sieved to give pellet sizes between 300 and 425 microns (40/50 mesh granules). The catalyst bed was supported on a bed of quartz glass wool. The reactor was operated under flowing hydrogen, and *n*-hexane (Aldrich, 99+% purity (<50 ppb sulfur, measured)) was added by infusion with a syringe pump (Sage model M365) through a T-junction prior to the reactor. In all experiments, the hydrogen/*n*-hexane ratio was kept at 6.0. Prior to reaction, the catalyst was slowly ramped in flowing hydrogen at 100 $cm^3$/min for 2 h to a temperature of 773 K and reduced *in situ* at 773 K in flowing hydrogen at 100 $cm^3$/min for 1 h. All reactions were conducted at 773 K, while the space velocity was varied to achieve different conversions and selectivities of products for study.

A purge-valve was used to send samples to a gas chromatograph/mass spectrometer (Hewlett Packard G1800A GCD System) for analysis. The gas chromatograph utilizes helium as the carrier gas and sends purged products of reaction through the column (HP-PLOT/$Al_2O_3$"S" Deactivated) to achieve product separation. Finally, products were ionized by the mass spectrometer, which incorporates an electron ionization detector (EID). A temperature ramp program provided the means for adequate peak separation in the GC column. To determine the signal/abundance ratio and quantify the concentration of each component in the products, normalization curves were obtained using pure compounds.

## RESULTS

### 1. *Catalytic Activity Measurements Using Sulfur-Free n-Hexane*

Several activity tests were conducted under sulfur-free conditions. The yields of the different products obtained at 773 K after 1.5 h on-stream over the three catalysts are summarized in Table 2. The differences between the product distribution obtained on Pt/KL and those on the nonzeolitic

**TABLE 2**

**Yields of Different Products Obtained at 773 K after 1.5 h On-Stream (WHSV: 5 $h^{-1}$)**

| Product | Pt/K L (IWI) | Pt/K L (VPI) | Pt/Mg(Al)O | Pt/$SiO_2$ | Equilibrium hexenes (for 0%–50% Bz yield) |
|---|---|---|---|---|---|
| Benzene | 45.69% | 48.68% | 4.59% | 13.82% | — |
| Methane | 4.65% | 3.12% | 0.40% | 4.03% | - |
| Ethane | 3.16% | 1.92% | 0.30% | 2.41% | - |
| Propane | 2.09% | 1.45% | 0.32% | 2.07% | - |
| Total hexenes: | 1.19% | 0.69% | 8.35% | 5.47% | 26–12.6% |
| *Trans*-3-hexene | 0.21% | 0.12% | 1.50% | 1.03% | 4.26–2.1% |
| *Trans*-2-hexene | 0.50% | 0.29% | 3.25% | 2.32% | 14–6.6% |
| 1-Hexene + *cis*-3-hexene | 0.23% | 0.13% | 1.77% | 1.00% | 4.20–2.0% |
| *cis*-2-hexene | 0.25% | 0.15% | 1.84% | 1.12% | 4.04–1.9% |
| 2,4 Hexadiene | 0.10% | 0.02% | 0.54% | 0.15% | - |
| Methylcyclopentane | 0.44% | 0.22% | 0.75% | 2.22% | - |
| 2-Methylpentane | 0.42% | 0.28% | 0.39% | 1.08% | - |
| Methylcyclopentenes | 0.31% | 0.11% | 1.20% | 2.06% | - |
| Cyclopentene | 0.23% | 0.15% | 0.42% | 0.75% | - |
| 3-Methylpentane | 0.12% | 0.12% | 0.14% | 0.38% | - |
| 1,3 Methylcyclopentadiene | 0.09% | 0.06% | 0.67% | 0.73% | - |
| 1,2 Dimethyl, *cis*-cyclopropane | 0.07% | 0.05% | 0.11% | 0.20% | - |

**TABLE 3**

**Yields of Different Products ($C_1$-$C_5$ Products Are Not Included) Obtained at the Same Overall Conversion (28%) at 773 K, $H_2$/*n*-Hexane Feed Ratio = 6.0**

| Product | Pt/K L | Pt/Mg(Al)O | $Pt/SiO_2$ |
|---|---|---|---|
| Benzene | 20.14% | 4.00% | 8.67% |
| Total hexenes | 3.28% | 10.48% | 5.20% |
| *Trans*-3-hexene | 0.43% | 1.81% | 0.91% |
| *Trans*-2-hexene | 1.34% | 4.28% | 2.11% |
| 1-Hexene + *cis*-3-hexene | 0.77% | 2.00% | 1.06% |
| *Cis*-2-hexene | 0.74% | 2.39% | 1.13% |
| Cyclopentene | 0.80% | 0.69% | 0.71% |
| Methylcyclopentenes | 0.75% | 2.33% | 1.37% |
| 1,3 Methylcyclopentadiene | 0.67% | 2.07% | 0.53% |
| Methylcyclopentane | 0.51% | 0.89% | 0.77% |
| 1,2 Dimethyl, *cis*-cyclopropane | 0.21% | 0.17% | 0.18% |
| 3-Methylpentane | 0.06% | 0.13% | 0.13% |
| 2-Methylpentane | 0.03% | 0.14% | 0.35% |

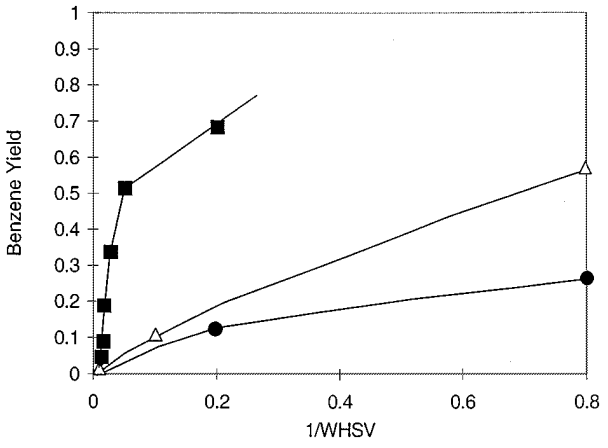


**FIG. 1.** Benzene yield as a function of reciprocal weight–hour space velocity at 773 K for the three catalysts investigated: Pt/KL (squares); $Pt/SiO_2$ (triangles); and Pt/Mg(Al)O (circles).

materials are clearly remarkable. For Pt/KL, the main product was benzene, with hexenes and lighter compounds as the principal by-products. By contrast, on the Pt/Mg(Al)O, the main products were hexenes. For comparison, the equilibrium yields of hexenes are included in Table 2. They vary with Benzene yield due to a change in $H_2$ partial pressure but they are always higher than the observed yields. Since it is well known that the benzene selectivity is a strong function of the overall conversion, we have made a similar comparison at the same total conversion (28%) for the three catalysts. This comparison is illustrated in Table 3, which does not include the $C_1$-$C_5$ products. Once again, Pt/KL exhibited a much higher benzene selectivity than Pt/Mg(Al)O and $Pt/SiO_2$. In addition to the products listed in Tables 2 and 3, a small fraction of condensation products ($C_6$+) were obtained with the $Pt/SiO_2$ and the Pt/Mg(Al)O catalysts. These products were not observed when the Pt/KL catalyst was employed. The superior performance of Pt/KL in comparison with the other two catalysts is further demonstrated in Fig. 1, which shows the overall initial benzene yield (extrapolated to zero time) as a function of the space time. The Pt/KL zeolite displayed the highest activity, while the Pt/Mg(Al)O was even less active than the $Pt/SiO_2$.

In the catalytic activity tests it was observed that, even in the absence of sulfur, all catalysts presented a moderate activity decay. To analyze the effect of catalyst deactivation on product distribution, the benzene and hexenes yields were measured as a function of time on-stream at several space velocities. Figures 2 and 3 make a comparison of the evolution of these yields on the Pt/KL and Pt/Mg(Al)O catalysts, respectively. A clear trend was observed. While the benzene yield decreased as a function of time, the hexene yield increased. This trend is less pronounced on the Pt/Mg(Al)O catalysts, on which the benzene yield is much lower at all times. For example, while on Pt/Mg(Al)O, the benzene yield dropped to less than 3% after 20 h on-stream, on Pt/KL, it remained above 20%, even after 70 h.

We have observed that when benzene and hexene selectivity data are plotted versus conversion, they all seem to lie on the same curves, regardless whether the conversion had been varied by letting the catalyst deactivate (time on stream) or by changing the space velocity. Figures 4 and 5 illustrate the selectivity curves for Pt/KL and Pt/Mg(Al)O, respectively. For both catalysts, the hexene selectivity is higher at low conversions while benzene dominates at high conversions. The important difference between the two catalysts is that on Pt/KL the selectivity to benzene begins to dominate at much lower conversions than on Pt/Mg(Al)O. From the mechanistic point of view, it is important to note that on both catalysts, benzene appears as a secondary product while hexene is an intermediate that eventually can be converted into benzene. This conversion is more clearly visualized in Fig. 6, which shows the variation of hexene yield versus benzene yield. It is clearly seen that, at low

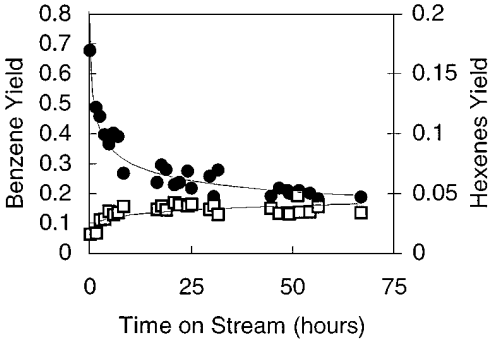


**FIG. 2.** Yield of benzene (full circles) and hexenes (open squares) as a function of time on stream (WHSV: 5 $h^{-1}$) on Pt/KL at 773 K. Note the scale change for hexenes.

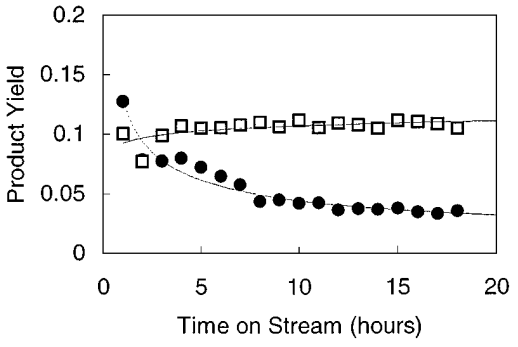


**FIG. 3.** Yield of benzene (full circles) and hexenes (open squares) as a function of time on stream (WHSV: 5 $h^{-1}$) on Pt/Mg(Al)O at 773 K.

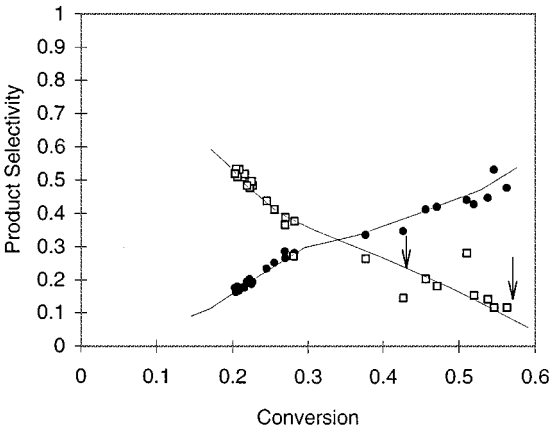


**FIG. 5.** Benzene (full circles) and hexenes (open squares) selectivities as a function of conversion on Pt/Mg(Al)O at 773 K. Conversion was varied by catalyst deactivation and by changing space velocity. Each arrow indicates the first data point in a new run at different space velocity.

conversions, both benzene and hexene yields are low and initially increase together, but as the benzene yield increases, the hexene yield goes through a maximum and then decreases. The behavior of Pt/KL is clearly different from that of the nonmicroporous catalysts. It is evident that Pt/KL is much more efficient in converting hexene into benzene than the other catalysts. At the high conversion end, both catalysts show high selectivity to benzene, although the activity for Pt/Mg(Al)O is significantly lower.

We have made no attempts in this work to optimize the preparation and performance of the (iwi) Pt/KL catalyst. For example, the addition of KCl, $CF_3Cl$, or back-exchange of ion-exchanged catalysts have been found to increase the benzene selectivity (23–25). Also, eliminating the traces of sulfur in the feed (26), could result in an important increase in activity and selectivity. Those changes would have only enhanced the great differences between Pt/KL and Pt/Mg(Al)O in favor of the Pt/KL.

For example, the hydrogenolysis activity of the Pt/KL prepared by IWI is higher than that of Pt/Mg(Al)O. However, this higher hydrogenolysis activity is not an intrinsic property of Pt/KL. The IWI procedure, as demonstrated by TEM, leaves a heterogeneous sample, with some larger clusters outside the channels of the zeolite. In order to achieve a more uniform distribution of small particles located inside the channels of the zeolite, a vapor phase impregnation technique by sublimation of $Pt(AcAc)_2$ was also carried out. In this case, the hydrogenolysis products were reduced as compared with the IWI catalyst, while aromatization activity was higher for all time onstream (Fig. 15). The methane yield on the VPI catalyst dropped from 3.1% at TOS = 1.5 h (Table 2) to 1.7% at TOS = 70 h.

### 2. *Catalytic Activity Measurements Using Sulfur-Containing n-Hexane*

To compare the effect of sulfur poisoning on the different catalysts, activity tests were conducted in the presence of controlled amounts of thiophene that resulted in a sulfur concentration of 0.6 ppm. Figure 7 shows the evolution of activity on the Pt/KL as a function of time on stream for sulfur-free and sulfur-containing feeds. As previously

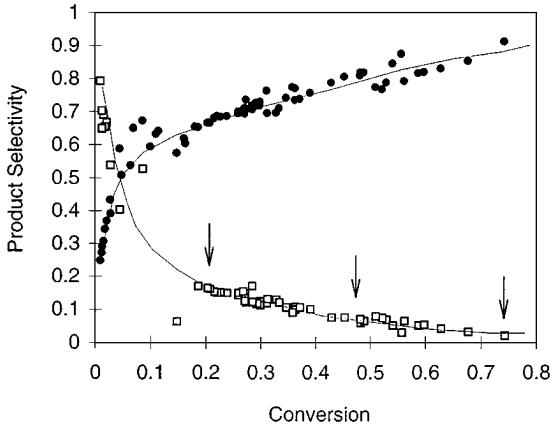


**FIG. 4.** Benzene (full circles) and hexenes (open squares) selectivities as a function of conversion on Pt/KL at 773 K. Conversion was varied by catalyst deactivation and by changing space velocity. Each arrow indicates the first data point in a new run at different space velocity.

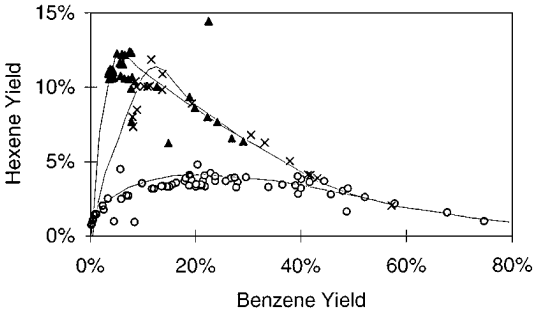


**FIG. 6.** Correlation between hexene yield and benzene yield for Pt/KL (open circles), Pt/Mg(Al)O (full triangles), and $Pt/SiO_2$ (crosses). The data were taken at 773 K, various space velocities, and various times on-stream.

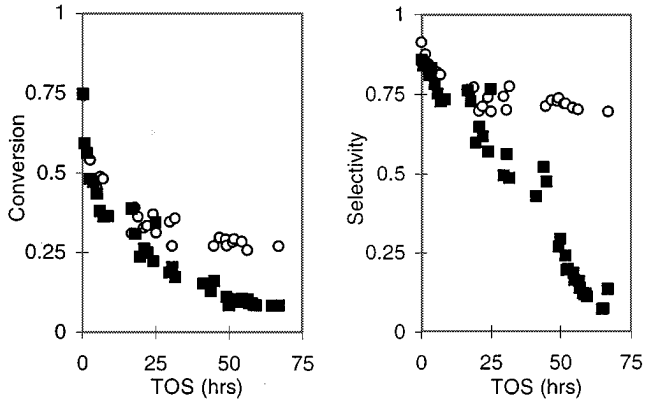


**FIG. 7.** Deactivation of the Pt/KL catalyst as a function of time on-stream at 773 K, using sulfur free (open symbols) and 0.6 ppm sulfur-containing (full symbols) feeds: (a) overall conversion; (b) benzene selectivity.

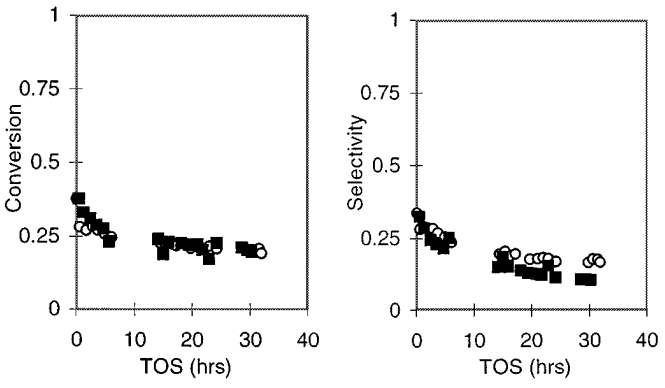


**FIG. 8.** Deactivation of the Pt/Mg(Al)O catalyst as a function of time on-stream at 773 K, using sulfur free (open symbols) and 0.6 ppm sulfur-containing (full symbols) feeds: (a) overall conversion; (b) benzene selectivity.

reported (28), a strong deactivation is seen for the run with 0.6 ppm sulfur. The deactivation was evident not only in the overall conversion but also in the benzene selectivity. By contrast, as shown in Fig. 8, the Pt/Mg(Al)O exhibited a much lower sensitivity to the presence of sulfur. In fact, both conversion and benzene selectivity were already low in the absence of added sulfur and the acceleration in deactivation by the addition of sulfur was only apparent in the benzene selectivity.

The most remarkable feature of the deactivation by sulfur is the increase in hexene selectivity. As shown in Table 4, the increase in hexene selectivity upon sulfur poisoning also occurs on Pt/Mg(Al)O and $Pt/SiO_2$ catalysts. However, the relative increases in hexene selectivity on these nonmicroporous catalysts are less pronounced than on Pt/KL.

When the benzene and hexene selectivities are plotted as a function of overall conversion (Fig. 9), the pattern observed for the poisoned Pt/KL becomes significantly different from that for the clean Pt/KL (Fig. 4). In fact, it begins to look like that of the non-microporous Pt/Mg(Al)O shown in Fig. 5. For instance, while the selectivity curves intersect at about 4–5% on the sulfur-free Pt/KL, they intersect at 35% on the Pt/Mg(Al)O catalyst. Under sulfur-containing feeds, the intersection of the curves for the Pt/KL catalyst shifts to higher conversions, i.e. about 16%.

The change in behavior of the Pt/KL catalyst under sulfur-containing feeds is also illustrated in Fig. 10, which shows the variation of hexene yield as a function of benzene yield. The figure includes the curves corresponding to data on sulfur-free Pt/KL and Pt/Mg(Al)O. It can be observed that, as the catalyst poisons, the hexene yield starts increasing until it reaches the curve corresponding to Pt/Mg(Al)O. From this trend, it could be said that the catalytic behavior of a poisoned Pt/KL catalyst looks similar to that of Pt/Mg(Al)O.

**TABLE 4**

**Effect of Sulfur-Poisoning on Product Selectivity Distribution after 30 h On-Stream at 773 K, $H_2$/*n*-Hexane Feed Ratio = 6.0**

| Product | Pt/KL | | Pt/Mg(Al)O | | $Pt/SiO_2$ | |
|---|---|---|---|---|---|---|
| | Nil S | 0.6 ppm S | Nil S | 0.6 ppm S | Nil S | 0.6 ppm S |
| Benzene | 74.97% | 57.69% | 17.57% | 10.18% | 36.79% | 23.57% |
| Total hexenes | 10.51% | 25.14% | 50.86% | 57.46% | 16.30% | 23.11% |
| *Trans*-3-Hexene | 1.54% | 4.34% | 8.42% | 10.14% | 2.96% | 4.42% |
| *Trans*-2-Hexene | 4.28% | 10.47% | 20.69% | 23.30% | 6.77% | 9.57% |
| 1-Hexene + *cis*-3-Hexene | 2.36% | 4.68% | 9.87% | 10.46% | 3.05% | 4.17% |
| *Cis*-2-Hexene | 2.33% | 5.66% | 11.89% | 13.56% | 3.52% | 4.94% |
| 1,3 Methylcyclopentadiene | 2.22% | 2.06% | 6.69% | 4.82% | 1.43% | 1.66% |
| Methylcyclopentenes | 2.58% | 4.48% | 6.36% | 7.65% | 4.89% | 6.31% |
| Methylcyclopentane | 1.60% | 4.58% | 2.86% | 3.51% | 5.24% | 9.24% |
| Cyclopentene | 2.71% | 0.99% | 1.45% | 0.73% | 1.72% | 1.22% |
| 1,2 Dimethyl, *cis*-cyclopropan | 0.72% | 0.28% | 0.43% | 0.20% | 0.42% | 0.31% |
| 3-Methylpentane | 0.22% | 0.82% | 0.28% | 0.34% | 0.52% | 1.27% |
| 2-Methylpentane | 0.14% | 0.74% | 0.18% | 0.23% | 1.58% | 3.68% |

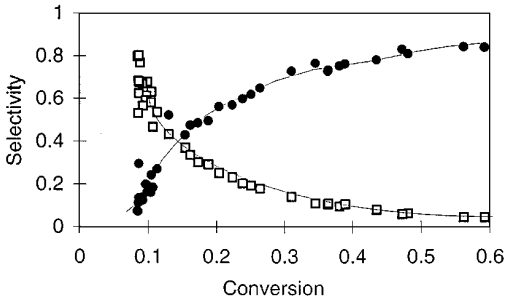


**FIG. 9.** Benzene (full circles) and hexene (open squares) selectivities as a function of conversion on Pt/KL at 773 K, in the presence of 0.6 ppm of sulfur.

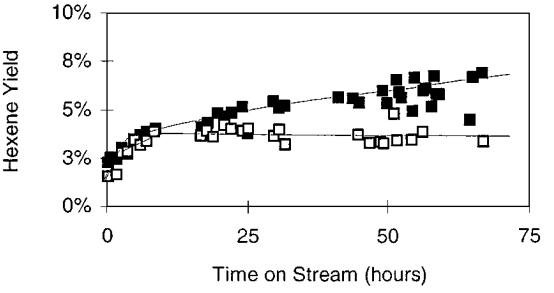


**FIG. 11.** Variation of hexene yield as a function of time on stream over the Pt/KL catalyst with (a) sulfur-free feed (open symbols) and (b) 0.6 ppm sulfur-containing feed (full symbols). (WHSV: 5 $h^{-1}$, $T =$ 773 K.)

It is instructive to compare the variation of hexene yield over the Pt/KL catalyst under sulfur-free and sulfur-containing feed conditions. This comparison is made in Fig. 11 that shows the evolution of hexene yield with time on stream for the two runs. It is observed that the rate of production of hexenes, not just the selectivity, increases as a result of the catalyst deactivation process. There is an important difference between the two runs. While in the sulfur-free case, the hexene yield increased during the first few hours on stream and then stabilized at about 3.5%, in the 0.6-ppm S run the hexene yield continued to increase for a much longer time and after 70 h had reached about 7.5% yield. As opposed to the trend exhibited by the production of hexenes, the production of methane paralleled that of benzene; that is, it decreased as a function of time on stream. It is interesting to see in Fig. 12 that the declines in benzene and methane production followed the same trend for both the sulfur-free and sulfur-containing runs.

### 3. *Physical Characterization of the Spent Catalysts*

The Pt catalysts on the three different supports were characterized by electron microscopy and X-ray absorption spectroscopy, as fresh samples and after reaction with sulfur-free or sulfur-containing feeds. It has been shown that an incipient wetness impregnation procedure similar to that used in this paper results in a large fraction of the Pt particles located inside the channels of the zeolite (27). The TEM analysis of the Pt/KL catalyst showed that, as expected, most of the platinum particles in the freshly reduced sample were too small to be observed at $2 \times 10^5$ magnification, and they are probably located inside the channels of the zeolite. However, some bigger particles were also observed. After 70 h of run with the clean *n*-hexane feed, most of the particles were still small with a small fraction of particles in the range of 15–20 nm. When the catalyst was exposed for 70 h to 0.6 ppm sulfur, particle growth was clearly evident, although a large fraction of small particles was still observed. The comparison of the two spent samples is illustrated in Fig. 13.

Platinum particle growth in the presence of sulfur is consistent with results reported by McVicker *et al.* (28). However, the corresponding EXAFS analysis on the same set of Pt/KL catalysts did not show a significant increase in Pt-Pt coordination number, which would parallel the

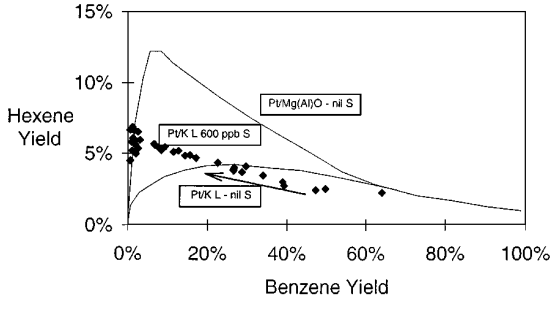


**FIG. 10.** Correlation between hexene yield and benzene yield for sulfur-poisoned Pt/KL. The arrow indicates the sequence in which the data were obtained as a function of time on-stream over a period of 67 h. The feed contained 0.6 ppm sulfur (full symbols). The two curves represent the data obtained on the sulfur-free runs reported in Fig. 6 for Pt/KL and Pt/Mg(Al)O, respectively.

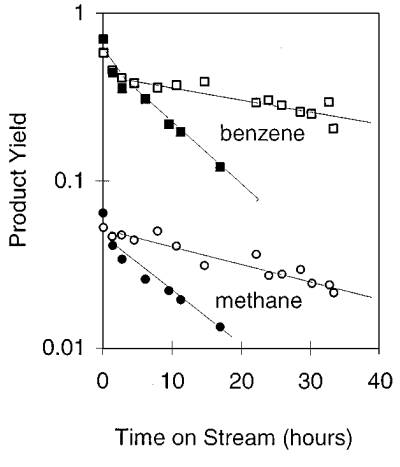


**FIG. 12.** Variation of benzene (squares) and methane (circles) yields as a function of time on-stream over the Pt/KL catalyst with (a) sulfur-free feed (open symbols) and (b) 5-ppm sulfur-containing feed (full symbols). (WHSV: 5 $h^{-1}$, $T = 773$ K.)

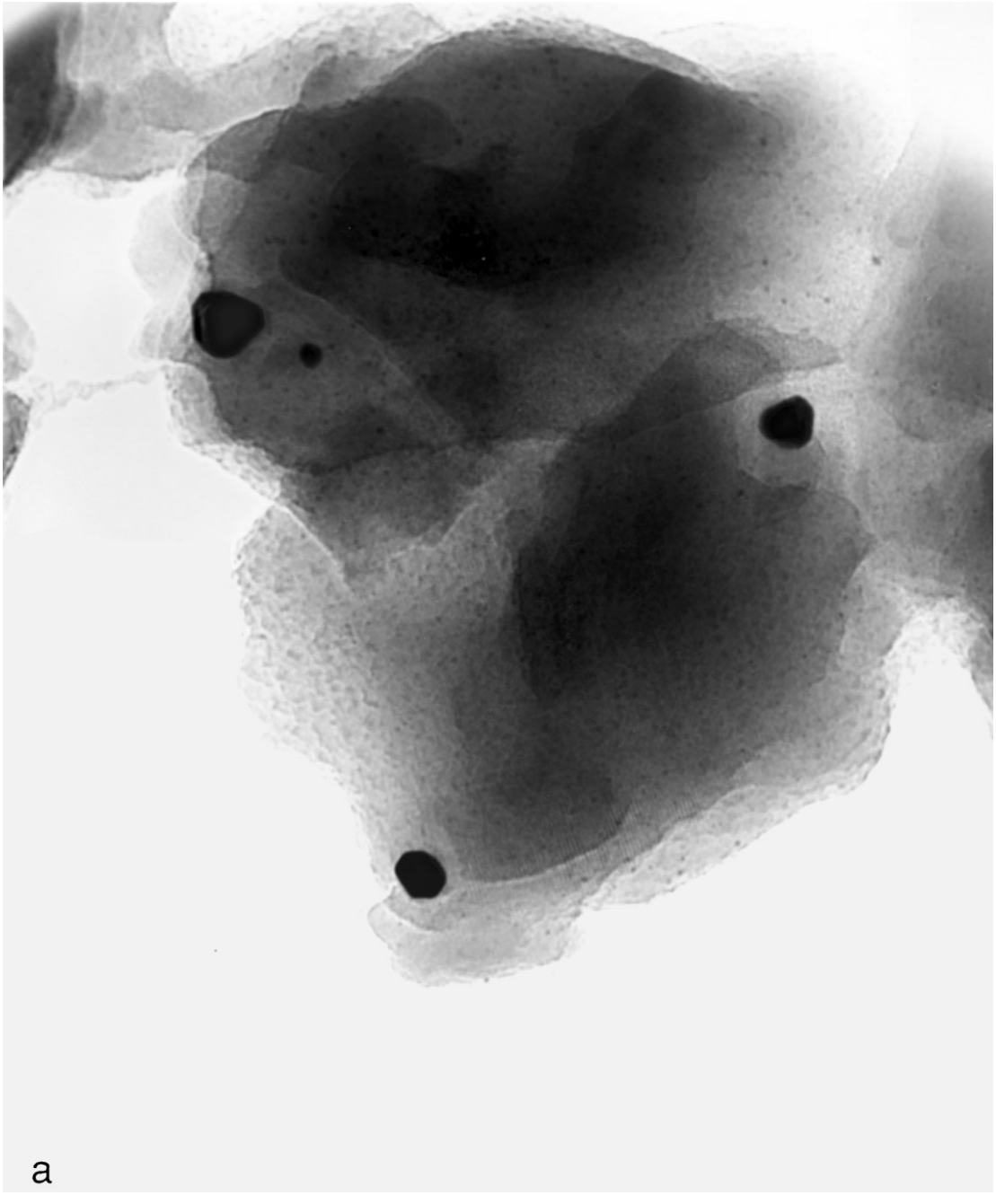


**FIG. 13.** TEM micrographs of Pt/KL catalyst after 70 h on-stream at 773 K: (a) sulfur-free conditions; (b) feed containing 0.6 ppm sulfur.

particle size increases observed by TEM. As shown in Fig. 14, the Fourier transforms of the sample run for 70 h under sulfur-free feed and that run under 0.6 ppm sulfur were very similar. Structural parameters were obtained by curve fitting analysis, using theoretical amplitude and phase functions for Pt-Pt, Pt-S, and Pt-O contributions obtained with the FEFF program. The results of the fit in the R-space are summarized in Table 6. The Pt-Pt coordination numbers for both spent catalysts were about 4, and close to the value of 3.7 reported before for a fresh Pt/KL catalyst (29). The catalyst spent in sulfur-containing feed exhibited a Pt-S coordination close to 1. The appearance of Pt-S coordination is in agreement with the results reported by Vaarkamp *et al.* (38) and implies that sulfur may be, at least partially, poisoning the Pt particles. No contribution of Pt-O bonds were predicted by the model calculations. When only Pt-Pt, or Pt-Pt and Pt-O contributions were used in the fit, the quality of the fitting was much lower than when Pt-S was included. It is interesting to note that a very small contribution of Pt-S was obtained in the fit of the sample spent with

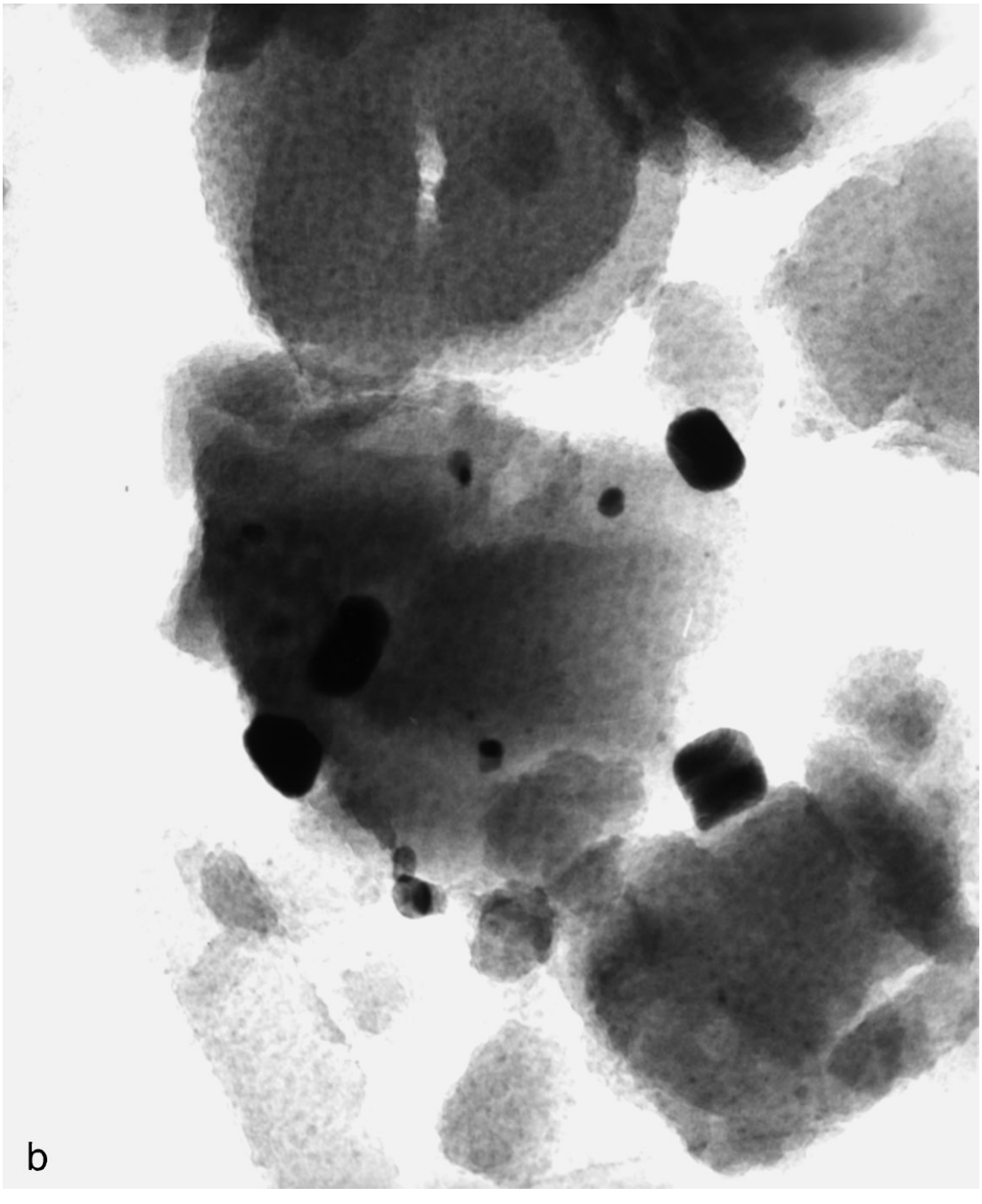


**FIG. 13**—*Continued*

the sulfur-free sample. This is not unreasonable considering that small traces of sulfur can be present in the feed and accumulate on the Pt surface over the 70-h run. They may be responsible for part of the deactivation observed in the "sulfur-free" runs.

TEM analysis (not shown) of the Pt/Mg(Al)O catalyst demonstrated that the platinum particles were significantly larger on the Mg(Al)O support than on KL. The fresh sample showed a large fraction of the particles with sizes of about 4 nm and a smaller fraction of larger particles ranging between 15 and 20 nm. No appreciable changes in size were detected after the run with clean *n*-hexane feed and only a slight growth after the run with the sulfur-containing feed. The EXAFS data are in good agreement with these observations (see Fig. 15). As shown in Table 6, the coordination number obtained for the sample exposed to sulfur-containing feed for 70 h was about the same as that of the fresh sample. Finally, the silica-supported catalyst exhibited particles smaller than 4 nm.

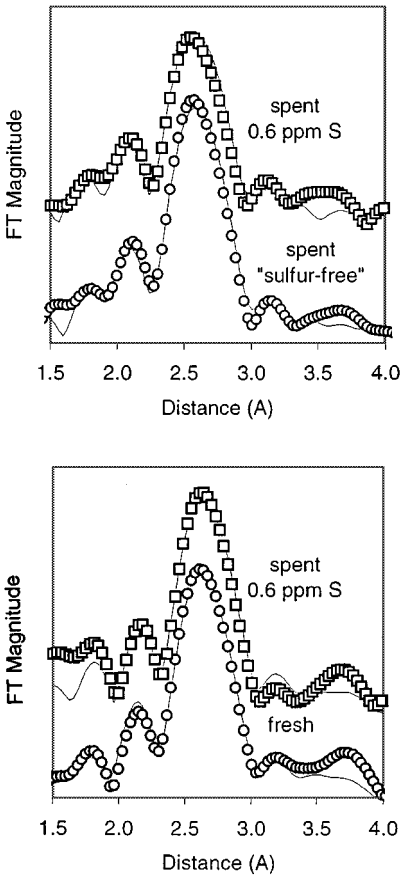


**FIG. 14.** Fourier transform (magnitude) ($k^3$, $\Delta k = 3.5$–$15$ Å$^{-1}$) of the EXAFS data obtained at liquid nitrogen temperature on *in-situ* reduced samples of: (a) Pt/KL catalyst: sample spent under sulfur-free conditions (circles) and sample spent under 0.6-ppm sulfur (squares); (b) Pt/Mg(Al)O catalyst: freshly reduced sample (circles) and sample spent under 0.6-ppm sulfur (squares). Solid lines are the fitting curves obtained using the parameters listed in Table 6.

## DISCUSSION

One of the first important conclusions of these results is that, in contrast with previous reports (14), Pt/Mg(Al)O is significantly less active and selective than the Pt/KL zeolite. This conclusion has crucial consequences, since it corroborates the exceptional ability of the Pt/KL catalyst and will eliminate the erroneous concept that only the basicity of the support was responsible for the high activity and selectivity of Pt/KL.

Our analysis of product distribution on the various catalysts investigated shows that the amount of hexenes produced in the *n*-hexane reaction is a good indication of the quality of the Pt/KL catalyst. That is, a well prepared Pt/KL catalyst should exhibit a very low selectivity to hexenes, even at moderate overall conversions. By contrast, a poorly prepared catalyst or a sulfur-poisoned catalyst results in a high selectivity to hexenes, and this selectivity only decreases at very high conversions. From this analysis we could

**TABLE 5**

**Comparation of Catalytic Activity of Pt/KL and Pt/Mg(Al)O**
**$H_2$/*n*-Hexane Feed Ratio = 6.0**

| Contact time (s) | Temperature (K) | Catalyst | Benzene yield | Reference |
|---|---|---|---|---|
| 3.35 | 773 | Pt/KL | 70% | This work |
| | | Pt/Mg(Al)O | 12% | This work |
| 3.50 | 750 | Pt/KL | 17% | (14) |
| | | Pt/Mg(Al)O | 15% | (14) |
| 0.7 | 773 | Pt/KL | 53% | This work |
| | | Pt/Mg(Al)O | 4% | This work |
| 1 | 750 | Pt/KL | 5% | (14) |
| | | Pt/Mg(Al)O | 4% | (14) |

infer that the comparative work of Pt/KL and Pt/Mg(Al)O catalysts (14) resulted in very similar catalytic properties because the Pt/KL sample employed in those early studies was not optimized. In that case, it was found that at an overall conversion near 40%, the hexene selectivity was the same for both catalysts. By contrast, our data indicate that on a well-prepared Pt/KL catalyst the selectivity to hexene is much lower than on Pt/Mg(Al)O. For example, at an overall conversion of 40%, the benzene/hexene yield ratios obtained in the present work are 7.3 and 1.8 for Pt/KL and Pt/Mg(Al)O, respectively. A similar comparison made from the data of Ref. (14) results in ratios of 2.7 and 2.5, respectively. Both results are close to the ratio of about 1.9, observed on our $Pt/SiO_2$ catalyst at the same overall conversion.

A similar conclusion can be drawn from the comparison of the activity level made on Table 5. The benzene yields reported on the early work for both Pt/KL and Pt/Mg(Al)O are about the same as those found in this work for Pt/Mg(Al)O. However, the yield reported on the present work over Pt/KL is significantly greater.

Even though it was early recognized that the *n*-hexane aromatization on Pt/KL would involve dehydrogenated

**TABLE 6**

**Structural Parameters Obtained from the Fitting of EXAFS Data Using Pt-Pt and Pt-S Theoretical References Developed with FEFF**

| | N | | R (nm) | | | $\sigma$ | |
|---|---|---|---|---|---|---|---|
| Catalyst | Pt-Pt | Pt-S | Pt-Pt | Pt-S | $\Delta E_o$ | Pt-Pt | Pt-S |
| Spent Pt/KL sulfur-free run | 4.3 | 0.2 | 0.282 | 0.230 | 2.7 | 0.0033 | — |
| Spent Pt/KL 0.6 ppm S run | 3.8 | 1.0 | 0.271 | 0.228 | 1.9 | 0.0036 | 0.0066 |
| Fresh Pt/Mg(Al)O | 8.7 | 0 | 0.275 | — | 7.8 | 0.0035 | — |
| Spent Pt/Mg(Al)O 0.6 ppm S run | 8.8 | 0.6 | 0.274 | 0.229 | 8.8 | 0.0035 | 0.0035 |

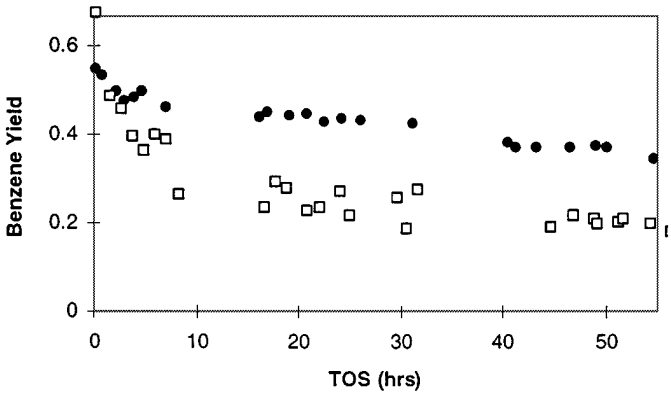


**FIG. 15.** Comparison of Pt/KL catalysts prepared by IWI (open squares) and VPI (full circles).

intermediates (9), only a few papers have paid attention to the role of hexenes (6). It must be noted that, as shown in Table 2, the hexane–hexenes equilibrium is not established. In all cases, the conversions to hexenes were much lower than the equilibrium conversions. However, the concentration of hexenes in the gas phase greatly changes from catalyst to catalyst. In fact, an analysis of the evolution of hexenes may provide important information about the state of the catalyst. For example, in agreement with the data from Manninger *et al.* (30, 31), our results indicate that hexenes are primary products, while benzene is essentially a secondary product. As these authors pointed out, hexenes as well as dienes and trienes are precursors for benzene on Pt (32, 33). A comparison of the observed trends on the different catalysts clearly shows that Pt is much more efficient in converting hexenes to benzene when supported on KL than when supported on $SiO_2$ or Mg(Al)O, but this ability is greatly reduced in the presence of sulfur. In previous work, conducted at conversions higher than 5%, benzene seemed to be a primary product (2). Our results show that on Pt/KL the conversion of hexene into benzene can only be noticed at very low conversions, i.e. <4%. Therefore, in a well-prepared Pt/KL benzene may appear as a primary product while, in fact, it is secondary.

The trends presented in this work indicate that Pt on all supports undergo the *n*-hexane dehydrogenation very easily. The exceptional aromatization activity of Pt/KL must then be explained in terms of its ability to convert hexene into benzene. To explain this we may refer to the interpretation of Iglesia and Baumgartner (10) who ascribed the high aromatization selectivity of this catalyst to its ability to resist coke formation. These authors have proposed that the high aromatization selectivity is intrinsic of clean Pt and the role of the KL zeolite is to inhibit bimolecular interactions that lead to coke formation. In support of this interpretation, calorimetric studies conducted by Sharma *et al.* (34) indicated that Pt/K(Ba)L exhibited similar heats of adsorption as those over Pt on an inert support such as $SiO_2$. However, after the *n*-hexane aromatization reaction, the carbon deposition on Pt/K(Ba)L resulted in a much lower suppression of adsorption sites than on $Pt/SiO_2$. These results clearly demonstrated the ability of Pt/KL to resist deactivation by coke.

Based on this interpretation and the trends in product distribution discussed above, one would conclude that on $Pt/SiO_2$ or Pt/Mg(Al)O the formation of coke would rapidly inhibit the Pt ability for converting hexenes to benzene. This coke, however, would have a much lower effect on the dehydrogenation activity, causing the observed increase in hexene selectivity on these catalysts. This can be easily explained in terms of required ensemble size. It is well known that the addition of inert metals to clean platinum surfaces results in strong modification of the product distribution in the conversion of *n*-hexane. For example, when Au-Pt surface alloys were made on Pt(111) single crystals, large decreases in *n*-hexane aromatization and hydrogenolysis rates were observed (35). These results demonstrate that the *n*-hexane aromatization reaction on Pt requires a relatively large ensemble of atoms. By contrast, the alkane dehydrogenation reaction is known to require a small number of metal atoms, perhaps as little as one (36), which would explain the resistance of the dehydrogenation function to deactivation. On the other hand, on KL the Pt particles would remain clean and conserve their aromatization capacity, consuming most of the hexene that is produced as a primary product.

In a recent TAP reactor investigation, Lafyatis *et al.* (37) have calculated turnover frequencies and selectivities for benzene formation on Pt/KL and Pt/Mg(Al)O. In that investigation they have found similar TOF and benzene/hexene ratios for both catalysts. However, since nonmicroporous catalysts lose their aromatization activity more quickly than microporous Pt/K L under reaction conditions due to coke formation, the TAP results conducted by sending small hydrocarbon pulses on a clean catalyst do not reflect the ability of the catalysts under reaction conditions. TAP reactors operate under conditions of Knudsen diffusion such that gas-phase collisions are minimized. Therefore, the effects of coking, which occur under reaction conditions, are deliberately suppressed.

The deactivation by sulfur requires further discussion. It has been proposed by McVicker *et al.* (28) and by Vaarkamp *et al.* (38) that, in the presence of sulfur, Pt particle growth is accelerated. Our TEM observations agree with those results but the EXAFS data did not show any metal particle growth. It is possible that the particle growth observed by TEM only reflects a growth of those particles located outside the zeolite channels, while the majority of the particles remain inside the channels and maintain a small size, even after 70 h in a sulfur-containing atmosphere. The next important issue that needs to be discussed is the cause for the observed shift in benzene and hexene selectivities in the

presence of sulfur. As mentioned in the previous section, the sulfided Pt/KL catalyst begins to behave as Pt/Mg(Al)O and $Pt/SiO_2$. One possible explanation is the migration of the metal particles from the interior of the zeolite channels to the outer surface (28, 38). That being the case, the metal particles in the outer surface would not be protected from coking and thus would lose their ability to aromatize the hexene. On the other hand, it is also possible that those particles remaining inside the channels may get partially poisoned by sulfur, even in minute concentrations, breaking up ensembles and losing their ability to aromatize (10). The parallel trends observed in Fig. 12 for the drops in the production of benzene and methane are in line with these concepts. They indicate that both aromatization and hydrogenolysis require a relatively large ensemble of atoms to constitute the active site.

If one analyzes the trend shown in Fig. 11 for the hexene yield as a function of time on-stream, one can see that, in the first run, the effect of coke alone results in a relatively rapid increase in hexene production followed by a long stability. This can be interpreted by a rapid coking of the Pt particles outside the zeolite. These coked particles would remain active only for hexene production while those inside continue making hexenes, which are rapidly converted to benzene.

In the second run, the combined effect of coke and sulfur would result in:

(a) an initial increase in hexene yield due to the coking of those particles outside the zeolite, and

(b) a longer-term increase in hexene production that could be due to two possible phenomena (i.e., slow migration of Pt particles, which subsequently get coked or slow sulfur poisoning inside the channels of the zeolite).

In both cases, the effect would be the same, a slow increase in hexene production and a decrease in benzene production. In a recent paper, Paal *et al.* (39) have shown that, while clean Pt blacks are active for *n*-hexane aromatization, they completely lose their aromatization activity after sulfidation treatments. After that treatment, only hexenes were observed as products. A similar behavior was observed on carbonized Pt blacks. These results fully agree with the proposal that both increased coke deposition on Pt outside the zeolite and sulfur poisoning are responsible for the deactivation of Pt/KL. The lower sensitivity to sulfur exhibited by the Pt/Mg(Al)O is also consistent with the proposed explanation. On this catalyst, the Pt particles do not have the protection of the microporous structure existing in the Pt/KL catalysts and, therefore, are rapidly poisoned by coke, even in the absence of sulfur. The addition of sulfur only causes a small additional deactivation. Regarding the potential of Pt/Mg(Al)O as a practical catalyst, its lower sensitivity to sulfur may not be enough to compensate for the low activity and selectivity that the catalyst has with or without sulfur.

A different interpretation has been recently offered by Fukunaga and Ponec (40). They have proposed that the presence of K inside the channels of the zeolite is responsible for the enhanced aromatization activity. This hypothesis has been supported by an increased aromatization observed when K was added as a promoter to a $Pt/SiO_2$ catalyst and it was followed by the conclusion that the effect of sulfur was not to poison the Pt, but rather to poison the K, making it lose its promoting effect. The fact that not only the benzene production, but also the methane formation rate, are greatly affected by the presence of sulfur (Fig. 12) would contradict this hypothesis, unless K is also a promoter for hydrogenolysis. In fact, Zaera and Somorjai (41), have found that the hydrogenolysis selectivity on Pt(111) increases by addition of K, although the hydrogenolysis rate decreases, as could be expected in a reaction that requires a large ensemble.

## CONCLUSIONS

In summary, this work has demonstrated that Pt/KL has a much higher activity and selectivity than Pt/Mg(Al)O or $Pt/SiO_2$ catalysts. It can be concluded that the basicity of the support alone cannot explain the high performance of Pt/KL catalysts for aromatization. The presence of hexenes as products which are generated in the reaction as precursors for benzene is an indication of the loss of aromatization activity. This loss may be brought about by the presence of a significant fraction of the metal particles outside the zeolite channels or by the partial poisoning of the metal surface. In most cases these two phenomena are interconnected, since the Pt particles outside the channels of the zeolite are more susceptible to coke formation and are rapidly deactivated. In the presence of sulfur some accelerated particle growth is observed. However, the pronounced deactivation may also be due to the deposition of small amounts of sulfur on the Pt particles outside and inside the zeolite, which effectively block and deactivate the large ensembles required for aromatization and hydrogenolysis. As a result, the selectivity to hexenes increases as the catalyst deactivates.

The IWI technique used is not the optimal preparation method for Pt/K L catalysts, because the resulting catalyst is heterogeneous and some large clusters remain outside the pores of the zeolite. These larger clusters are more active for hydrogenolysis than are those found on Pt/Mg(Al)O. Better Pt/K L catalysts can be prepared by vapor phase impregnation methods, resulting in more homogeneous distributions of small Pt clusters inside the channels of the zeolite. These catalysts result in decreased hydrogenolysis activity and remarkably higher aromatization activity.

## ACKNOWLEDGMENTS

This work was supported by the Oklahoma Center for the Advancement of Science and Technology (OCAST). We acknowledge the National Science Foundation for a GRT traineeship for one of us (GJ) and Phillips

Petroleum for a scholarship. We also acknowledge the technical support of Greg Strout from the OU S. R. Noble Electron Microscopy Laboratory for TEM measurements, the personnel at Brookhaven National Lab for the EXAFS experiments, and Dr. Walter E. Alvarez (INTEMA) for helpful discussions.

## REFERENCES

1. Bernard, J. R., *in* "Proc. 5th Internat. Zeolite Conf." (L. V. C. Rees, Ed.), p. 686. Heyden, London, 1980.
2. Lane, G., Modica, F. S., and Miller, J. T., *J. Catal.* **129**, 145 (1991).
3. Hughes, T. R., Buss, W. C., Tamm, P. W., and Jacobson, R. L., *Stud. Surf. Sci. Catal.* **28**, 725 (1986).
4. Tamm, P. W., Mohr, D. H., and Wilson, C. R., *Stud. Surf. Sci. Catal.* **38**, 335 (1988).
5. Rotman, D., *Chem. Week*, **8**, Feb. 26 (1992).
6. Davis, R. J., *Heterog. Chem. Rev.* **1**, 41 (1994).
7. Tauster, S. J., and Steger, J. J., *J. Catal.* **125**, 387 (1990).
8. Besoukhanova, C., Guidot, J., and Barthomeuf, *J. Chem. Soc. Faraday Trans. I* **77**, 1595 (1981).
9. Derouane, E. G., and Vanderveken, D. J., *Appl. Catal.* **45**, L15 (1988).
10. Iglesia, E., and Baumgartner, J. E., *in* "Proc. X Internat. Congr. Catal (L. Guczi *et al.*, Eds.) p. 993. Elsevier Sci., New York, 1993.
11. Iglesia, E., and Baumgartner, J. E., *in* "Proc. IX Internat. Zeolite Conf., Montreal, 1992."
12. Larsen, G., and Haller, G. L., *Catal. Lett.* **3**, 103 (1989).
13. Mielczarski, E., Hong, S. B., Davis, R. J., and Davis, M. E., *J. Catal.* **134**, 359 (1992).
14. Davis, R. J., and Derouane, E. G., *Nature* **349**, 313 (1991). [*Ibid.*, *J. Catal.* **132**, 269 (1991)]
15. Miller, J. T., Agrawal, N. G. B., Lane, G. S., and Modica, F. S., *J. Catal.* **163**, 106 (1996).
16. Schaper, H., Berg-Slot, J. J., and Stork, W. H. J., *Appl. Catal.* **54**, 79 (1989).
17. Cavani, F., Trifirio, F., and Vaccari, A., *Catal. Today* **11**, 173 (1991).
18. Alvarez, W. E., and Resasco, D. E., *J. Catal.* **164**, 467 (1996).
19. Sayers, D. E., and Bunker, B. A., *in* "X-ray Absorption: Principles, Applications, Techniques of EXAFS, SEXAFS, and XANES" (D. Koningsberger and R. Prins, Eds.), p. 211. Wiley, New York, 1988.
20. Rehr, J. J., Zabinsky, S. I., and Albers, R. C., *Phys. Rev. Lett.* **69**, 3397 (1992).
21. Rehr, J. J., Mustre de Leon, J., Zabinsky, S. I., and Albers, R. C., *J. Amer. Chem. Soc.* **113**, 5135 (1991).
22. Mustre de Leon, J., Rehr, J. J., Zabinsky, S. I., and Albers, R. C., *Phys. Rev. B* **44**, 4146 (1991).
23. Dai, L-X., Sakashita, H., and Tatsumi, T., *Chem. Lett.*, 387 (1993).
24. Larsen, G., and Haller, G. L., *Catal. Today* **15**, 431 (1992).
25. Sugimoto, M., Katsuno, H., Hayasaka, T., Ishikawa, N., and Hirasawa, K., *Appl. Catal. A* **102**, 167 (1993).
26. Sugimoto, M., Murakawa, T., Hirano, T., and Ohashi, H., *Appl. Catal. A* **95**, 257 (1993).
27. Ostgard, D. J., Kustov, L., Poeppelmeier, K. R., and Sachtler, W. M. H., *J. Catal.* **133**, 342 (1992).
28. McVicker, G. B., Kao, J. L., Ziemiak, J. J., Gates, W. E., Robbins, J. L., Treacy, M. M. J., Rice, S. B., Vanderspurt, T. H., Cross, V. R., and Ghosh, A. K., *J. Catal.* **139**, 48 (1993).
29. Vaarkamp, M., van Grondelle, J., Miller, J. T., Sajkowski, D. J., Modica, F. S., Lane, G. S., Gates, G. C., and Koningsberger, D. C., *Catal. Lett.* **6**, 369 (1990).
30. Manninger, I., Zhan, Z., Xu, X. L., and Paal, Z., *J. Mol. Catal.* **66**, 223 (1991).
31. Manninger, I., Zhan, Z., Xu, X. L., Tetenyi, P., and Paal, Z., *Appl. Catal.* **51**, L7 (1989).
32. Paal, Z., and Tetenyi, P., *J. Catal.* **30**, 350 (1973).
33. Dautzenberg, F. M., and Plateeuw, J. C., *J. Catal.* **19**, 41 (1970).
34. Sharma, S. B., Ouraipryvan, P., Nair, H. A., Balaraman, P., Root, T. W., and Dumesic, J. A., *J. Catal.* **150**, 234 (1994).
35. Sachtler, J. W. A., and Somorjai, G. A., *J. Catal.* **81**, 77 (1983).
36. Biloen, P., Dautzenberg, F. M., and Sachtler, W. H., *J. Catal.* **50**, 77 (1977).
37. Lafyatis, D., Froment, G. F., Pasau-Claerbout, A., and Derouane, E. G., *J. Catal.* **147**, 552 (1994).
38. Vaarkamp, M., Miller, J. T., Modica, F. S., Lane, G. S., and Koningsberger, D. C., *J. Catal.* **138**, 675 (1992).
39. Paal, Z., Matusek, K., and Muhler, M., *Appl. Catal.* **149**, 113 (1997).
40. Fukunaga, T., and Ponec, V., *J. Catal.* **157**, 550 (1995).
41. Zaera, F., and Somorjai, G. A., *J. Catal.* **84**, 375 (1983).